Available online at www.sciencedirect.com
SCIENCE DIRECT®
ELSEVIER
Earth and Planetary Science Letters 216 (2003) 619–634
EPSL
www.elsevier.com/locate/epsl

Quantification of the factors controlling the presence of excess ^{40}Ar or ^{4}He

Ethan F. Baxter *

Department of Earth Sciences, Boston University, 685 Commonwealth Avenue, Boston, MA 02215, USA

Received 28 February 2003; received in revised form 8 September 2003; accepted 18 September 2003

Abstract

A quantitative physical model is presented which includes the factors that control the presence, or absence, of internally derived excess ^{40}Ar or excess ^{4}He in geological systems. In particular, the model incorporates the transport and partitioning properties of the rock surrounding the mineral of thermochronologic interest and illuminates the related effects on the amount of excess ^{40}Ar or ^{4}He preserved in the system. Modeling of a simplified 1-D rock column bounded by an external sink for ^{40}Ar or ^{4}He shows that a steady-state excess ^{40}Ar or ^{4}He profile develops, the magnitude of which is determined by a system parameter called the 'transmissive timescale', τ_T. The characteristic time required to reach this steady state depends upon τ_T and the 'total local sink capacity', TLSC, wherein the important role of local matrix mineral and fluid phases is incorporated. Together, these two system parameters (τ_T and TLSC) determine the evolution of excess ^{40}Ar or ^{4}He buildup within a system above the closure temperatures of all minerals involved. An analytical expression for the 1-D system describing the evolution of excess ^{40}Ar (or by analogy ^{4}He) in a particular potassium-bearing (or U–Th-bearing) mineral located at a distance, L, from an external sink has been derived empirically from model results:

$$^{40}Ar_{age-equivalent}(L,t) \cong \frac{\tau_T^{Ar}}{2}\left(1-\exp\left(\frac{5}{2}\frac{t}{\tau_T^{Ar}(1+TLSC^{Ar})}\right)\right)$$

Local matrix minerals, perhaps most notably quartz, may act as important sinks for ^{40}Ar (except in the most fluid-rich systems where fluids dominate) and thus are fundamental in controlling, and limiting, thermochronologically problematic excess ^{40}Ar in neighboring potassium-bearing minerals. In general, the model provides a rigorous means of predicting excess noble gas content, residence, release, and transport within the compositionally variable and thermally evolving crust.

1. Introduction

Noble gas-based geochronometers ($^{40}Ar/^{39}Ar$ and U–Th/He) represent the most widely used and applicable method of constraining the thermal, tectonic, and geomorphic evolution of the crust and surface of the Earth [1–4]. Standard models for thermochronology [5] consider only the physical properties (i.e. volume diffusivity, grain size, etc.) of the mineral to be dated, as well as the cooling rate, to determine the time

* Tel.: +1-617-358-2844; Fax: +1-617-353-3290.
E-mail address: efb@bu.edu (E.F. Baxter).

0012-821X/03/$ – see front matter © 2003 Elsevier B.V. All rights reserved.
doi:10.1016/S0012-821X(03)00541-7

(and temperature) interval over which the mineral 'closes' and quantitative retention of in situ produced, radiogenic daughter isotope begins. This highlights an advantage of noble gas-based thermochronometers over other decay systems such as Rb/Sr or Sm/Nd: namely, that standard practice is to model diffusive loss of ^{40}Ar or ^{4}He from the source mineral with a zero surface concentration boundary condition (cf. [2,5]) or, by implication, to assume the mineral is surrounded by an effectively 'infinite reservoir' (cf. [6–8]) thus preventing the buildup of problematic excess ^{40}Ar or ^{4}He in the mineral of interest, and permitting age analysis of a single mineral (rather than requiring analysis of mineral–whole rock pairs). No reservoir is truly infinite so, in practice, the requirement is that the surroundings of the mineral behave enough like an infinite reservoir so as to prevent significant radiogenic ^{40}Ar or ^{4}He buildup in the mineral of interest before its closure. The success of ^{40}Ar/^{39}Ar thermochronology, in particular, in producing geologically consistent ages corroborated by independent methods, shows that the infinite reservoir assumption must hold in many environments.

The disadvantage of noble gas based thermochrometers is that when this 'infinite reservoir' assumption does not hold, excess ^{40}Ar, or by analogy excess ^{4}He, is the result. Excess ^{40}Ar – the 'longstanding bane of K/Ar geochronology' ([1], p. 130) – is a common and problematic aspect of thermochronologic interpretation which causes an age inferred by the standard assumptions to be too old (it remains to be seen if excess ^{4}He is similarly notorious, though reports do exist [2]). Aside from assuming an infinite reservoir exists, the standard model does not consider the immediate surroundings into which radiogenic ^{40}Ar or ^{4}He is released *before* that source mineral closes, though broadly similar effects have been considered for other isotopic systems (e.g. [9–12]).

This contribution presents a physical model that illuminates the characteristics of the entire geologic system which control the presence or absence of excess ^{40}Ar or ^{4}He. Two fundamental system parameters: (1) a transmissive timescale, τ_T (cf. [6]), and (2) a 'total local sink capacity', TLSC (defined for either Ar or He), describe how well the 'infinite reservoir' assumption is met, and thus control the amount and evolution of excess ^{40}Ar or ^{4}He. Ultimately, this paper arrives at an empirically derived analytical expression for excess ^{40}Ar or ^{4}He in a particular mineral of thermochronological interest. The analytical solution is particularly useful in that it simplifies the system of model equations such that the role of key physical parameters is illuminated and easily assessed for a given geologic system. With this quantitative framework, we can not only better understand how and where excess argon may occur, but also use it to glean further information about the characteristics of the environment within which it was produced. While this paper will focus on the ^{40}Ar/^{39}Ar system, the principles and equations are directly analogous and applicable to the U–Th/He thermochronometer and, in principle, applications involving fissiogenic Xe and Kr [13]. Finally, while primarily designed for geochronologic applications, the model is also of use in applications of noble gas geochemistry requiring a quantification of where and when excess radiogenic noble gases are stored (and thus may also be released) within subduction environments [14], the mantle [15], and the thermally and petrologically evolving crust [13].

2. Past work

There are several ways in which 'excess Ar' has been defined (e.g. [1,8]), often carrying connotations to its inferred origins. Here, for the case of slowly cooling crustal systems, excess Ar will be referred to as any non-atmospheric ^{40}Ar (i.e. ^{40}Ar in excess of atmospheric proportions to ^{36}Ar; atmospheric ^{40}Ar is easily corrected for and is thus ignored in this paper) which is *not* the result of in situ radiogenic ^{40}Ar* accumulation within K-bearing minerals due to diffusional closure of the mineral. This therefore includes any locally derived (indeed, even in situ derived) radiogenic ^{40}Ar introduced into the minerals of the system *before their respective closure*. The definition of excess Ar used here is similar to 'extraneous Ar' defined in [1], however, here, radiogenic Ar de-

rived in situ (and remaining) in minerals before closure is considered to be excess Ar.

There have been countless reports of excess Ar (for a review, see [1,8]), but often it is ignored or avoided, for in most instances the goal is to obtain meaningful geochronological information, and in this regard, excess Ar is not useful. However, several studies have considered the occurrence of excess Ar and proposed explanations for its occurrence [6,8,16–21]. A common theme of these explanations is that excess Ar reflects a high ambient ^{40}Ar partial pressure, and, consequently, some means of creating and sustaining such elevated local levels of ^{40}Ar during system evolution. It has been suggested that systems within which Ar is unable to migrate sufficiently fast will lead to the buildup of locally derived excess Ar in minerals [6,15,20]. Thus, the rate of Ar migration out of local systems has been identified, and modeled, as a key factor in controlling excess Ar (see [6] and Section 3.1). The importance of pore fluids in accommodating Ar and its migration has also been emphasized [6–8,12,13]. However, in the most recent models of excess Ar [6,8], the important role of other local minerals has not been adequately considered. The advance of the modeling in this paper over [6,8] is a more complete and generalized quantitative description of excess Ar evolution including: (1) open-system behavior and escape of Ar to an 'external' sink, (2) the integrated effect of local pore fluid and matrix mineral sinks for Ar, and (3) a range of mineral–fluid (or generally, mineral–ITM, see Section 3.1) exchange mechanisms. The model represents an advance over broadly similar models for oxygen isotope [9,10] and Rb/Sr isotope [11,12] systems by incorporating both the effects of radiogenic production and open-system transport both of which are essential to noble gas based thermochronometric interpretation.

3. Potential sinks for Ar

To rigorously evaluate the 'infinite reservoir' assumption we must begin by identifying the potential sinks for radiogenic ^{40}Ar in a system. Fig. 1 depicts the potential sinks, including both external and internal (or local) sinks. The combined effectiveness of the external and internal sinks determines how well the 'infinite reservoir' assumption is satisfied.

3.1. External sinks and the 'transmissive timescale'

Ultimately, the macroscale external sink for Ar, or any volatile, is the atmosphere. There are also external sinks on a meso-scale that, relative to neighboring systems, may behave as effective reservoirs or conduits for Ar leading ultimately to the atmospheric reservoir. For example, a regional shear zone may exhibit enhanced fluid flow and permit rapid escape of noble gases to the surface (though advecting fluids may also introduce excess Ar; see Section 4.1).

The ability for a geologic system to mediate escape of Ar to an external sink has been accounted for by a parameter called the transmissive timescale, τ_T [6]. τ_T is defined as the characteristic

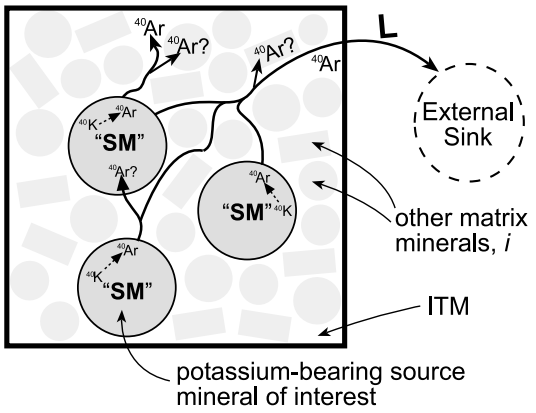

Fig. 1. Cartoon of potential sinks for Ar. ^{40}Ar produced radiogenically in a particular potassium-bearing source mineral of thermochronologic interest, 'SM', may escape that mineral above its diffusive closure temperature, upon which it may: (1) leave the system at some rate via the ITM to some external sink (such as the atmosphere) located a distance 'L' away, (2) remain in the local ITM, (3) re-enter or simply remain in 'SM' as thermochronologically problematic 'excess Ar', or (4) enter local matrix minerals. The effectiveness of the external sink depends on the transmissive timescale, τ_T. The effectiveness of the local sinks depends on their diffusive closure properties, relative modes, and Ar partition coefficients (i.e. TLSC). The volume of ITM is greatly exaggerated in this figure.

time required for ^{40}Ar produced within a particular potassium-bearing source mineral of interest (this mineral is referred to herein as 'SM' or by the subscript 'sm') to escape from the local system to some external sink for ^{40}Ar, located a distance L away. τ_T therefore depends on the mechanism for Ar transport through the system. For Ar transport by bulk diffusion through the intergranular transporting medium (ITM) [cf. 22], which may be a static pore fluid, dry grain boundaries, or some combination of the two:

$$\tau_T = \frac{L^2 M_{sm} K_{sm}}{D_{ITM}} = \frac{L^2}{D^*_{sm}} \quad (1)$$

(from [6]), where variables are as defined in Table 1.

Table 1
Definitions of terms

a	radius of mineral grain (m)
$C_{K,n}$	^{40}K concentration in mineral n (mol g^{-1})
C_{ITM}	^{40}Ar concentration in the ITM (mol g^{-1})
$C_{n,age-equiv}$	^{40}Ar age-equivalent concentration in mineral n (yr); see Eq. 9
$C_{n(edge)}$	^{40}Ar concentration at the outer edge radial increment of mineral grain, n (mol g^{-1})
C_n	average ^{40}Ar concentration in mineral n (mol g^{-1})
D_{ITM}	diffusivity of Ar in the ITM with tortuosity (usually a factor of 1.0–0.7) correction (m^2 yr^{-1})
D_n	solid state diffusivity of Ar in mineral n (m^2 yr^{-1})
i (subscript)	denotes matrix minerals other than the source mineral of interest
K_n	equilibrium partition coefficient for Ar between mineral, n, and ITM (see Eq. 2)
L	characteristic lengthscale of 1-D rock column system (m)
M_n	$\rho_n m_n / \rho_{ITM} \phi$, mass ratio of mineral, n, to ITM
m_n	volume fraction (i.e. mode) of mineral, n
r	radius of a mineral (m)
sm (subscript)	denotes potassium bearing ^{40}Ar-source mineral of interest, SM
t	time (yr)
TLSC	total local sink capacity; see Eq. 3
x	spatial coordinate in 1-D rock column (m)
ϕ	volume fraction of the ITM, i.e. porosity
λ_K	5.810×10^{-11} yr^{-1}, effective decay constant for ^{40}K decay to ^{40}Ar (yr^{-1})
ρ_{ITM}	density of ITM (g cm^{-3})
ρ_n	density of mineral, n (g cm^{-3})
τ_T	transmissive timescale; see Eq. 1

For Ar transport by an advecting fluid, $\tau_T = L/v^*$, where v^* is defined similarly to D^* above. Advective transport, localized in shear zones or fractures [6,23–25], may be orders of magnitude more efficient in transporting Ar than bulk diffusion. However, at some lengthscale, bulk diffusion must be the limiting factor for Ar to reach such effective external sinks. Thus, one must consider the diffusive transport properties over the distance, L, to the nearest effective external sink. The equations and modeling that follow focus on bulk diffusive transport of noble gases.

3.2. Local sinks and the TLSC

Matrix mineral or fluid phases could also serve as *local* sinks for Ar – or at least sequester some of the excess ^{40}Ar that might otherwise be incorporated back into SM. The capacity of a matrix mineral or fluid depends on how strongly it partitions Ar and how much of the phase is present. A sink mineral must also be diffusively 'open' to permit Ar entry. Ultimately, any lithologic unit with a large total local sink capacity (TLSC; see below), comprising the capacities of all matrix minerals, fluids, and grain boundaries, will exhibit relatively little excess Ar in its SM, and may act as an effective external sink for neighboring lithologies with a smaller TLSC and/or a larger τ_T.

The equilibrium distribution of ^{40}Ar produced from all K-bearing minerals (including SM) will be governed by the equilibrium partition coefficients for Ar [6,8,18]. Since in a given system, all phases share the same ITM (if the rock is treated as a continuum and a representative averaging volume of rock is chosen so as to exceed fine scale variations in ITM characteristics: a necessary simplification for the modeling), let us express the partition coefficients for Ar for a mineral, n, as:

$$K_n = \frac{C_n}{C_{ITM}} \quad (2)$$

where C_n is the concentration of Ar in the mineral, n, at equilibrium, and C_{ITM} is the concentration in the local ITM. In a closed system at equilibrium, such as may characterize higher temperature portions of the crust [16,20] or mantle [21],

these partition coefficients, along with the mineral modes (m_n) and ITM porosity (ϕ), determine the distribution of Ar. The product M_nK_n, for a given mineral, n, is the ratio of the amount of Ar (or ^{40}Ar) between that mineral and the ITM at equilibrium. If M_nK_n is a large number, then most of the Ar is partitioned into that mineral as opposed to the local ITM. If $M_nK_n \ll 1$, then the ITM itself behaves as an effective sink for ^{40}Ar with respect to that mineral. Ratios of MK between matrix minerals (M_iK_i) and SM ($M_{sm}K_{sm}$) will describe similarly to what extent matrix minerals may act as effective sinks for Ar with respect to SM.

Summing the individual sink capacities of all local phases relative to SM, we may define TLSC thus as:

$$\mathrm{TLSC} = 1/(M_{sm}K_{sm}) + \sum_i M_iK_i/(M_{sm}K_{sm}) \qquad (3)$$

TLSC is the equilibrium ratio between the Ar stored in the rest of the local system to the Ar stored in SM. For example, when TLSC = 1, the total Ar content of the local system is split exactly 50/50 between SM and the rest of the system. When TLSC $\ll 1$, local sink capacity is negligible and any excess ^{40}Ar in the system will be located in SM – an undesirable situation for thermochronology. When TLSC $\gg 1$, the converse is true. Note that TLSC comprises *both* the local fluid and matrix mineral capacities.

4. Model system

The modeling in this paper will focus on the geologic system depicted in Fig. 2. The model system consists of a 1-D column of rock with uniform characteristics throughout. The rock consists of any number of minerals, each of which possesses its own intrinsic characteristics including: Arhennius Ar diffusion parameters, grain size and shape, m_n, ^{40}K content ($C_{K,n}$), and K_n. By definition, $C_{K,sm} \neq 0$. Matrix minerals may or may not have potassium. The ITM of the rock column has a spatially and temporally constant ϕ and D_{ITM}. The length of the rock column is L.

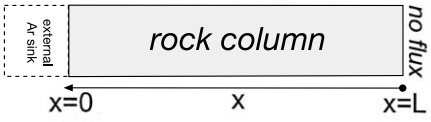

Fig. 2. Model 1-D geologic system used. D_{ITM}, ϕ, m_n, K_n, are constant throughout the rock column. At every point along the column, the rock may be envisioned as shown in Fig. 1.

4.1. Boundary and initial conditions

For all modeling, the boundary and initial conditions are the same. An external sink is located at one end of the column of rock and a fixed, zero ^{40}Ar concentration boundary condition is applied there. The other end of the column is assigned a no-flux boundary condition, and thus may be envisioned as the half spacing between two equal external sinks. The initial condition is zero radiogenic ^{40}Ar concentration in all phases, and the ITM everywhere. All radiogenic ^{40}Ar is generated during the simulation from the potassium-bearing minerals. In natural systems, radiogenic ^{40}Ar inherited from in situ pre-metamorphic production may also be significant in raising the initial ^{40}Ar contents. Such a non-zero initial condition is easily incorporated into the model equations, but is not dealt with here.

It is also possible in nature that the external sink may be a unit, such as a shear zone, through which distally derived radiogenic ^{40}Ar is continuously supplied. Such a non-zero ^{40}Ar boundary condition will simply add a baseline to the characteristic ^{40}Ar profile within the rock column which may simply be added or subtracted in interpretation. A time-varying boundary condition, also conceivable in natural systems, would more seriously complicate the system and is not dealt with here.

4.2. Governing equations

All terms are as defined in Table 1. At each node (from $x = 0$ to $x = L$) along the 1-D column (Fig. 2), three dependent variables must be accounted for: (1) the ^{40}Ar concentration in the ITM, (2) the ^{40}Ar concentration in SM, and (3) the ^{40}Ar concentration in each of the matrix minerals, i. Any non-atmospheric ^{40}Ar incorpo-

rated in the system above the closure temperature of the phases involved is, by definition, excess ^{40}Ar.

4.2.1. Equation for ^{40}Ar in the ITM

At each point in the system, the flux of ^{40}Ar into the local ITM consists of three components: (1) the bulk diffusive flux (F_D) from adjacent nodes in the rock column, (2) the flux from local SM (F_{sm}), and (3) the flux from the other local matrix minerals (F_i):

$$F_{ITM} = F_D + F_{sm} + \sum_i F_i \tag{4}$$

The change in ^{40}Ar concentration in the ITM (C_{ITM}) may be expressed as follows:

$$\frac{\partial C_{ITM}}{\partial t} = D_{ITM}\frac{\partial^2 C_{ITM}}{\partial x^2} - M_{sm}\cdot\left(\frac{\partial C_{sm}}{\partial t} - \lambda_K C_{K,sm}\right) - \sum_i M_i\left(\frac{\partial C_i}{\partial t} - \lambda_K C_{K,i}\right) \tag{5}$$

The first term on the right accounts for bulk diffusion of ^{40}Ar through the ITM (Fick's 2nd law). The second and third terms account for local exchange of ^{40}Ar with each mineral. Each of the terms in parentheses accounts for the concentration change in each mineral caused by exchange with the local ITM thus excepting that which is due purely to in situ radiogenic production. These terms are scaled by M_n, to account for the net effect on C_{ITM}. $C_{K,n}$ are treated as constant, which results in negligible errors for durations less than 100 Myr.

4.2.2. Equations for ^{40}Ar in minerals

These equations can have a variety of forms depending on the mechanism of the exchange between each mineral and the ITM. Exchange may be modeled as volume diffusion (with cylindrical, spherical or more complicated grain geometry), dissolution–precipitation, or by assuming instantaneous exchange to equilibrium. Let us first deal with the equilibrium case. This would be analogous to any system wherein all phases are well above their nominal closure temperatures, thus permitting free and full exchange of Ar and the constant maintenance of equilibrium even in an evolving system. This is a good assumption for higher temperatures (say, >500°C) as most common minerals (i.e. mica [1,26], feldspar [1], amphibole [27], quartz [28]) are diffusively 'open' to Ar at these conditions (see Section 5.4 for a discussion of where this assumption theoretically breaks down). Thus, under the assumption of local equilibrium exchange for Ar, equations for C_n may be written (after [29]):

$$\frac{\partial C_n}{\partial t} = (K_n C_{ITM} - C_n) + \lambda_K C_{K,n} \tag{6a}$$

The first term accounts for the instantaneous exchange of ^{40}Ar between mineral and ITM as the system adjusts to equilibrium, defined by K_n. The second term accounts for radiogenic production. The equation for dissolution–precipitation-controlled exchange [29] is similar to Eq. 6a only with a fractional reaction rate, $R_n < 1$:

$$\frac{\partial C_n}{\partial t} = R_n(K_n C_{ITM} - C_n) + \lambda_K C_{K,n} \tag{6b}$$

For exchange limited by volume diffusion out of (or into) minerals, as is employed in thermochronologic models, the equation for radial diffusion in a mineral, n, for all interior radial increments, j, is [30]:

$$\frac{\partial C_{(n,j)}}{\partial t} = D_n\frac{\partial^2 C_{(n,j)}}{\partial r^2} - \frac{zD_n}{r}\cdot\frac{\partial C_{(n,j)}}{\partial r} + \lambda_K C_{K,n} \tag{7}$$

where $z=1$ for cylindrical or disk-shaped minerals like micas, and $z=2$ for spherical geometry, more appropriate for plagioclase or quartz. In Eq. 7, $C_{(n,j=\text{surface})} = K_n\cdot C_{ITM}$ for the effective concentration in the ITM at the surface of each mineral. $\partial C_n/\partial t$ for use in Eq. 5 may be calculated from Eq. 7 by summing cylindrical or spherical shells.

For all numerical simulations presented in this paper, Eq. 7 for the diffusional exchange mechanism was used. Note that for high temperatures when mineral diffusivities are sufficiently rapid, the use of Eq. 6a (equilibrium case) or Eq. 7 (diffusive exchange) produces identical results (i.e. $C_n = C_{(n,j)}$). Using Eq. 7 allows for simulations of slowly decreasing temperature where minerals each gradually pass through their closure and the system behavior may no longer be modeled as equilibrium.

4.3. High temperature–equilibrium model: non-dimensionalization

Before proceeding with the model, it is useful to recast the equations for the equilibrium case in terms of non-dimensional variables. Let:

$$x' = x/L \quad C'_{\mathrm{ITM}} = K_{\mathrm{sm}} C_{\mathrm{ITM}} \quad t' = D_{\mathrm{ITM}} t/L^2$$

and recall:

$$\tau_{\mathrm{T}} = \frac{L^2 M_{\mathrm{sm}} K_{\mathrm{sm}}}{D_{\mathrm{ITM}}}$$

Inserting Eq. 6a into Eq. 5 and substituting these variables yields:

$$\frac{\partial C'_{\mathrm{ITM}}}{\partial t'} = \frac{\partial^2 C'_{\mathrm{ITM}}}{\partial x'^2} - \tau_T (C'_{\mathrm{ITM}} - C_{\mathrm{sm}}) - \sum_i \tau_{\mathrm{T}} \frac{M_i}{M_{\mathrm{sm}}} \left(\frac{K_i}{K_{\mathrm{sm}}} C'_{\mathrm{ITM}} - C_i \right) \quad (8a)$$

$$\frac{\partial C_{\mathrm{sm}}}{\partial t'} = \frac{\tau_{\mathrm{T}}}{M_{\mathrm{sm}} K_{\mathrm{sm}}} (C'_{\mathrm{ITM}} - C_{\mathrm{sm}} + \lambda_{\mathrm{K}} C_{\mathrm{K,sm}}) \quad (8b)$$

$$\frac{\partial C_i}{\partial t'} = \frac{\tau_{\mathrm{T}}}{M_{\mathrm{sm}} K_{\mathrm{sm}}} \left(\frac{K_i}{K_{\mathrm{sm}}} C'_{\mathrm{ITM}} - C_i + \lambda_{\mathrm{K}} C_{\mathrm{K},i} \right) \quad (8c)$$

These equations show that, for the equilibrium case, the system behavior is governed solely by the fundamental parameters that were already identified: τ_{T}, M_n and K_n (where M_n and K_n are the parameters that define TLSC). Potassium contents ($C_{\mathrm{K},n}$) are also a factor but may be accounted for by expressing excess Ar as an 'age equivalent' (see Section 5.1).

5. Modeling results

Numerical simulations of ^{40}Ar evolution in the rock column, using the equations above, were performed with a FORTRAN90 code written by the author. An explicit finite difference numerical scheme was employed with variable spatial step size (finer nearest the external sink). This code allows for arbitrary variations in any of the intrinsic mineral properties, temperature–time histories, and spatial variations in modes of source and sink minerals. As formulated, porosity must remain constant in space and time, but other ITM properties (K, D_{ITM}) may be varied. All simulations described in this paper include a single source mineral of interest (subscript sm) with disc shaped geometry (appropriate for a mica) and fixed mode and any number of other matrix minerals, i, with either disc-shaped or spherical geometry and fixed mode.

5.1. Definition of '^{40}Ar age equivalent'

A convenient way to express the amount of excess ^{40}Ar in any of the system components is as an 'age equivalent'. ^{40}Ar age equivalent (denoted $C_{\mathrm{age-equiv}}$) thus has units of time. $C_{\mathrm{age-equiv}}$ is the age represented by the amount of ^{40}Ar in the mineral of interest with reference to the amount of potassium in that mineral. For example, the definition of $C_{\mathrm{sm,age-equiv}}$ reduces to the familiar age equation:

$$C_{\mathrm{sm,age-quiv}} = \frac{1}{\lambda_{\mathrm{K}}} \ln \left(1 + \frac{C_{\mathrm{sm}}}{C_{\mathrm{K,sm}}} \right) \quad (9)$$

This simplified age equation for K/Ar, and the use of constant $C_{\mathrm{K},n}$ in the simulations, results in insignificant errors except for durations greater than about 100 Myr.

5.2. 'Steady-state' Ar evolution above mineral closure temperatures: equilibrium case

Multiple runs were conducted for different values of K_n, M_n, and D_{ITM}, all at constant temperatures well above the closure of any of the system minerals (i.e. the equilibrium case). Modeling reveals that after a characteristic amount of time has elapsed, the system reaches a 'steady-state' distribution of ^{40}Ar within the mineral phases, and ITM, across the rock column (Fig. 3). The steady state reflects the balance between radiogenic production of ^{40}Ar within potassium-bearing minerals, and bulk diffusive loss of ^{40}Ar to the external sink from the model rock column.

Model simulations revealed that two fundamental characteristics of this steady-state profile are related to τ_{T} and TLSC. First, the amount of excess ^{40}Ar within a sink mineral located at a distance $x = L$ from the external sink is a direct function of τ_{T}. Specifically, for the boundary conditions used here, once steady state is achieved:

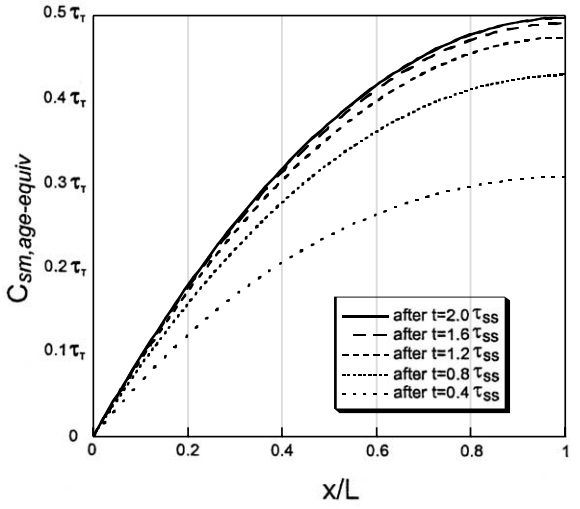

Fig. 3. Evolution of excess ^{40}Ar (age-equiv) within the source mineral as a function of distance in the model rock column and time. Each curve represents the ^{40}Ar profile at a different time during system evolution, where time is parameterized by τ_{SS}. Ultimately, a steady-state profile is approached. Model results here are for temperatures maintained well above the closure of all minerals (i.e. the equilibrium case).

$C_{sm,age-equiv(L)} = \tau_T/2$ (Fig. 3). This steady state, once reached, is a function only of τ_T, regardless of the absolute values of any of the parameters that define it (i.e. K_{sm}, M_{sm}, L, D_{ITM}) or TLSC.

Second, the characteristic time required to approach the steady-state profile is an exponential function (see Eq. 11) of a parameter denoted τ_{SS}, defined in terms of τ_T and TLSC as:

$$\tau_{SS} = \tau_T\left(1 + 1/M_{sm}K_{sm} + \sum_i M_iK_i/M_{sm}K_{sm}\right) = \tau_T(1 + TLSC) \quad (10)$$

Here the functional importance of the local matrix minerals, i, is evident. The effect of varying TLSC is shown in Fig. 4. For TLSC $\ll 1$, local sink capacity is negligible and $\tau_{SS} = \tau_T$ and the system evolves to steady state more rapidly. For TLSC $\gg 1$, τ_{SS} increases, slowing the evolution of the system to the steady state prescribed by τ_T as the significant local reservoir of minerals and ITM takes longer to 'fill up'.

Finally, the potassium content of the matrix minerals (if non-zero) will have an effect on $C_{sm,age-equiv}$. The greater the potassium content of matrix minerals ($\Sigma_i\ M_iC_{K,i}$) relative to the potassium content in SM ($m_{sm}C_{K,sm}$), the greater $C_{sm,age-equiv}$ (see Eq. 11). This simple relationship is valid only in the equilibrium case. Similar effects of bulk rock potassium content on locally derived excess ^{40}Ar have been noted in the past [16].

5.3. Empirically derived analytical expression for excess Ar

Based on systematic evaluation of the empirical results of the modeling – encompassing over 60 simulations for a wide range of system parameters (τ_T ranged from 300 to $>40\,000\,000$ yr wherein D_{ITM}, M_{sm}, ϕ and K_{sm} were varied; TLSC ranged from <0.01 to >4000 wherein ϕ, and M_n and K_n were varied) – the relations between $C_{sm,age-equiv}$ (at distance $x = L$), τ_T, TLSC, and potassium contents have been successfully formulated into a single empirically derived analytical solution:

$$C_{sm,age-equiv}(L,t) \cong \frac{M_{sm}C_{K,sm} + \sum_i M_iC_{K,i}}{M_{sm}C_{K,sm}} \cdot \frac{\tau_T}{2} \left(1 - \exp\left(\frac{5}{2} \cdot \frac{t}{\tau_T(1 + TLSC)}\right)\right) \quad (11)$$

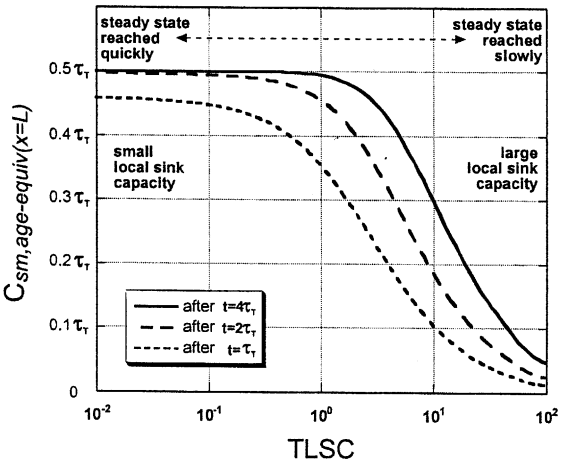

Fig. 4. Evolution of excess ^{40}Ar (age-equiv) in the source mineral located at a distance L within the rock column as a function of TLSC. Model results here are for temperatures maintained well above the closure of all minerals (i.e. the equilibrium case).

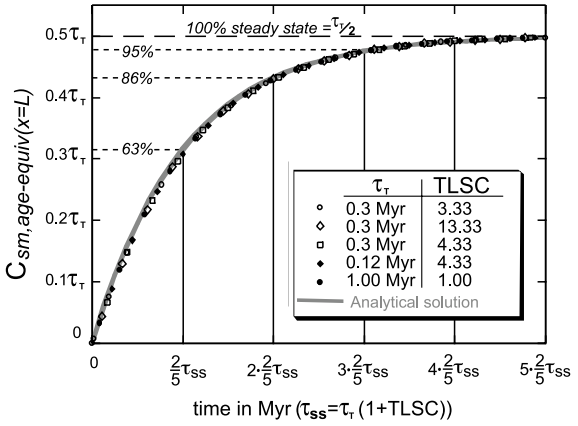

Fig. 5. Evolution of excess ^{40}Ar (age-equiv) in the source mineral located at a distance L within the rock column. Time is shown in units of $(2/5)\tau_{SS}$ to illuminate the exponential term in Eq. 12. The quality of the analytical solution (Eq. 12) is shown by excellent agreement with five representative numerical model simulations with a range of geologically feasible τ_T and TLSC. Dotted lines indicate the percent attainment of the steady state. Model results here are for temperatures maintained well above the closure of all minerals (i.e. the equilibrium case).

Note that if the only potassium-bearing mineral is the source mineral of interest, SM (i.e. all $C_{K,i}=0$) then Eq. 10 reduces to:

$$C_{\mathrm{sm,age-equiv}}(L,t)\cong$$

$$\frac{\tau_T}{2}\left(1-\exp\left(\frac{5}{2}\cdot\frac{t}{\tau_T(1+\mathrm{TLSC})}\right)\right) \qquad (12)$$

Also recall that, at equilibrium, $C_{sm}=K_{sm}C_{ITM}=(K_{sm}/K_i)C_i$. Eq. 11 incorporates both of the key attributes observed from modeling: (1) that the steady-state $C_{sm,age-equiv}$ (pre-exponential factor) is equivalent to $\tau_T/2$, and (2) that the time required to reach steady state is a function of τ_T and TLSC. The 5/2 factor was determined empirically, and is appropriate for the boundary and initial conditions (described in Section 4.1) of the model rock column. Fig. 5 shows the empirically derived analytical solution as compared to five representative numerical simulation results, showing a range of parameters, from which the analytical solution was established. The analytical solution holds for all τ_T and TLSC so long as local equilibrium is maintained by adequately fast mineral diffusivities (see below).

5.4. Breakdown of Eq. 11: the issue of local equilibrium

If temperatures cool and various minerals pass through their closure intervals, a threshold is approached below which local equilibrium is no longer maintained between system phases and the analytical solution (Eq. 11) and Eqs. 8a and 8b are no longer adequate to describe further system evolution. To examine this threshold quantitatively, let us consider the simple case of diffusional exchange with a cylindrical source mineral. The following equations, derived in [6] in terms of the same non-dimensional variables as in Section 4.3, illuminate the mathematics of mineral–ITM exchange for this case:

$$\frac{\partial C'_{\mathrm{ITM}}}{\partial t'}=\frac{\partial^2 C'_{\mathrm{ITM}}}{\partial x'^2}-\mathrm{De}_{\mathrm{sm}}\cdot\frac{(C'_{\mathrm{ITM}}-C_{\mathrm{sm(edge)}})}{\delta r'} \qquad (13)$$

and

$$\frac{\partial C_{\mathrm{sm(ave)}}}{\partial t'}=$$

$$\frac{\mathrm{De}_{\mathrm{sm}}}{M_{\mathrm{sm}}K_{\mathrm{sm}}}\cdot\frac{(C'_{\mathrm{ITM}}-C_{\mathrm{sm(edge)}})}{\delta r'}+\frac{\tau_T}{M_{\mathrm{sm}}K_{\mathrm{sm}}}\lambda_K C_K \qquad (14)$$

where De, a 'diffusive exchange' parameter [6,29], is:

$$\mathrm{De}_{\mathrm{sm}}=\frac{2D_{\mathrm{sm}}L^2}{a_{\mathrm{sm}}^2D^*_{\mathrm{sm}}}=\frac{2D_{\mathrm{sm}}\tau_T}{a_{\mathrm{sm}}^2} \qquad (15)$$

where D^*_{sm} is defined in Eq. 1, and $\delta r'$ is a non-dimensional radial increment in the cylindrical mineral ($\delta r'=r/a$), and $C_{sm(edge)}$ is the concentration at the very outermost radial increment in the mineral. De is the ratio between τ_T and the timescale for local diffusive exchange between the mineral and the ITM. As shown in Fig. 6, when $\mathrm{De}_{sm}>15$ the source mineral diffusively exchanges fast enough with the ITM such that local equilibrium is maintained everywhere. For $\mathrm{De}_{sm}<15$ equilibrium breaks down as the bulk diffusive transport via the ITM is too fast compared to the local diffusive exchange rate.

In realistic geologic settings, there are physical upper limits on D^* imposed by finite ϕ), and D_{ITM} (also, see Section 7). Thus, in nature the most relevant situation where De drops significantly is

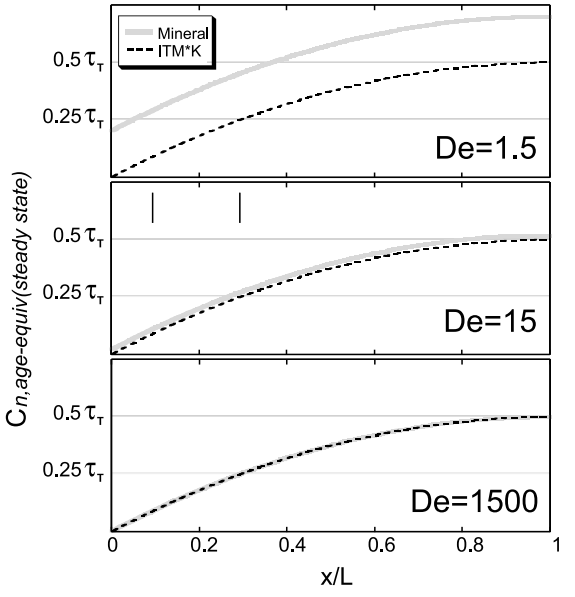

Fig. 6. Excess ^{40}Ar (age-equiv) at steady state in a system mineral and the ITM as a function of De. ITM ^{40}Ar content is scaled by K such that equilibrium is indicated when the two lines coincide, as in the bottom panel. For De smaller than 15, disequilibrium results between the local ITM and the mineral, at which point Eqs. 6a, 8, 11, 12 are no longer valid.

when mineral D_n drop due to decreasing temperatures. Let us then move beyond the steady-state equilibrium case and consider simulations into lower temperatures as the various system minerals themselves begin to close.

5.5. *Mineral closure and the effectiveness of sink minerals*

The overall evolution of the system may be arbitrarily divided into three segments: (1) the time before a steady state is reached, (2) the time between attainment of steady state and SM closure, and (3) the time after SM closure as the system cools to surface temperatures. Note that the divisions between these time intervals are fuzzy as neither are instantaneous events. Consider also that the modeling here is for uniform grain dimensions for each phase. In nature, grain sizes of a particular mineral will surely vary within a rock. Such grain size variation simply has the effect of further widening the interval of mineral

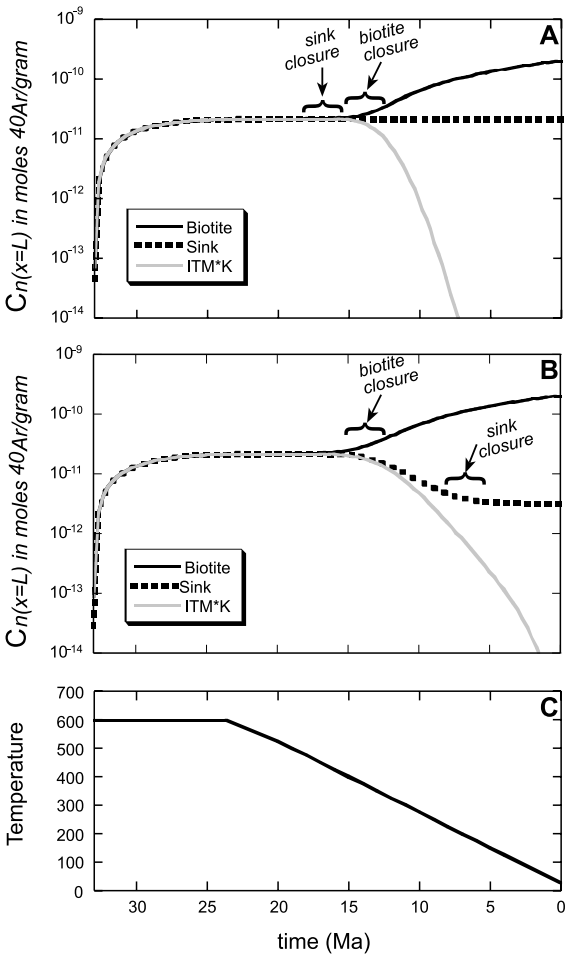

Fig. 7. Evolution of ^{40}Ar contents of ITM, source mineral, and a sink mineral. ITM ^{40}Ar content is scaled by K. The source mineral is biotite and $m_{biot} = 0.1$, and $C_{K,biot} = 2.4 \times 10^{-7}$ mol g^{-1}. Diffusion parameters for biotite are: $D^0 = 236$ m^2 yr^{-1} and $Q_a/R = 23700$ [26]. Both A and B follow the T–t history shown in C. The sink mineral in both A and B also has $m = 0.1$ and $K_{sink} = K_{biot}$. The remaining 80% of the rock is ignored (i.e. it neither houses nor produces ^{40}Ar). τ_T throughout both simulations is 3 Myr. The amount of excess Ar at steady state is $\sim 2 \times 10^{-11}$ mol g^{-1} (1.5 Ma excess), equivalent to $\sim 10\%$ of the measured age today. (A) Sink mineral with higher closure temperature than biotite: $D^0 = 2.36$ m^2 yr^{-1} and $Q_a/R = 23700$. Cylindrical sink mineral has $a = 400$ μm. (B) Sink mineral with a lower closure temperature than biotite. Here, the diffusion parameters for quartz [28] were used: $D^0 = 1.89 \times 10^{-11}$ m^2 yr^{-1} and $Q_a/R = 5700$. Spherical sink mineral has $a = 100$ μm. This sink mineral emulates quartz only in terms of its closure properties (quartz partitioning effects are shown in Fig. 9).

closure. Such effects are easily incorporated into the model by monitoring intramineral ^{40}Ar contents for each grain size separately.

If temperatures decrease before the steady state is reached, and any of the matrix minerals in the system begin to close, this will cause an acceleration of the ramp-up in C_{sm} due to a decrease in TLSC (Fig. 4). Such a case could correspond to matrix minerals with relatively high closure temperatures such as amphibole [27]. Another interesting effect could arise from ongoing mineral reactions creating a mineralogy with different TLSC (for example, consuming a mineral with small K and replacing it with one of larger K). In such a scenario, TLSC could increase or decrease leading to deceleration or acceleration of the approach to steady state.

Remember that the partitioning characteristics of the matrix minerals do not affect the steady state C_{sm} (Eq. 11), only the time required to reach it. Thus, *once steady state is reached*, any of the non-potassium bearing matrix minerals may close diffusively, but these changes will have no effect on the steady-state profile in C_{sm} or C_{ITM}. A matrix mineral which closes during the steady-state time segment will preserve its ^{40}Ar content associated with that steady state (Fig. 7A).

Once SM has closed to further exchange, then C_{sm} is locked in, and for the purposes of that SM of interest, the story is over. At this point a main source of ^{40}Ar (or the sole source if $C_{K,i} = 0$) to the rest of the system is shut off. However, for the matrix minerals that are still open, the story continues. C_i of the matrix minerals themselves, may prove useful by: (1) elucidating the system properties (namely, TLSC and τ_T) during lower temperature evolution, and (2) predicting the amount of excess ^{40}Ar contained in the SM. Matrix minerals which close after SM may lose some of the ^{40}Ar that they housed during the steady-state time. This could be the case for matrix minerals with relatively low closure temperatures, such as quartz [28], which may close at as low as ~150°C (depending strongly on the cooling rate given its very low activation energy). The amount of ^{40}Ar that such a matrix mineral will lose by the time we can sample and analyze it at the surface depends on two factors: (1) how long it remains open after SM has closed (Fig. 7B), and (2) the τ_T of the system *with reference to the matrix mineral* of interest during this cooling interval (Fig. 8). The system τ_T (particularly the characteristics of the ITM, and the spacing, L, between effective external Ar sinks) may change upon cooling as rocks become more brittle, closely spaced fractures may form (favoring shorter τ_T), fluids may be exhausted (favoring longer τ_T) or reorganized. Field evidence for a drop in τ_T with cooling beyond ~350°C has been documented in at least one locality [6]. Even if a matrix mineral remains open and *could* 'leak' its accumulated ^{40}Ar into the local ITM and out of the system, the extent to which this is possible depends on τ_T.

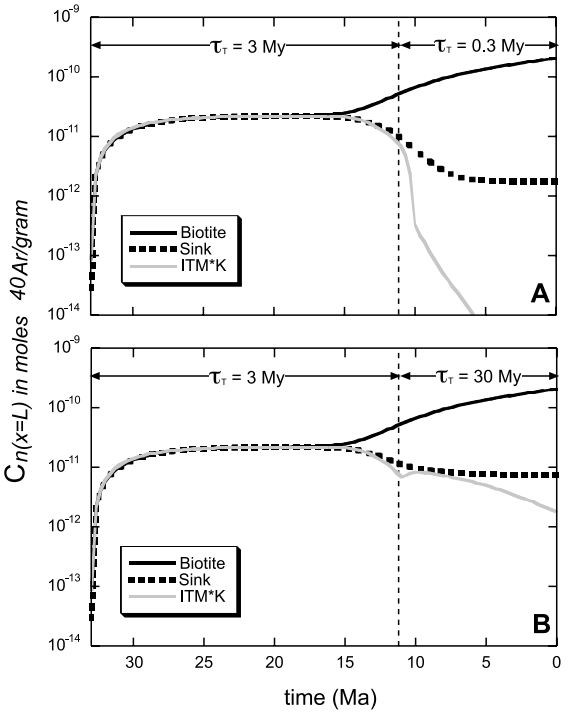

Fig. 8. Evolution of ^{40}Ar contents of ITM, source mineral, and a sink mineral with 'quartz'-like diffusivity (as in Fig. 7B) where system τ_T changes after source mineral closure. Other parameters are the same as in Fig. 7B. (A) τ_T drops to 0.3 Myr after biotite closure, resulting in significant loss of ^{40}Ar from ITM and, thus, from 'quartz' sink as well. (B) τ_T increases to 30 Myr, resulting in comparatively little loss of ^{40}Ar from the ITM, and the 'quartz' sink.

6. Local sink phases in natural systems

To evaluate the effectiveness of minerals or fluids in real systems, we must consider their modes and Ar partitioning. The mode effect (including the 'mode' of fluid: i.e. porosity) is straightforward, and of course may vary from one rock to another. Recently summarized experimental data shows that fluids partition Ar 10^3–10^6 times more strongly than most minerals clearly demonstrating the potential for fluids to act as an effectively infinite sink for Ar in the crust [8]. Thus, fluids will surely dominate the Ar budget in any system *if* they are present in sufficient quantity. But fluids exist only in minute quantities in the crust (metamorphic porosity may range between 10^{-5} and 10^{-3}; [31–33]), and are essentially absent in dry systems such as may characterize many ultra-high pressure environments [20,34]. In such conditions, Ar will begin to partition back into the minerals of the system – but into which minerals? This depends on the relative partitioning between the system minerals.

Data on Ar partitioning (which may be extracted from relative Ar solubility data) between minerals is limited, though some important recent advances have been made [8]. While the reader is referred to [8] for a review of silicate Ar partitioning data, here let us focus on two key minerals: biotite, which is a common potassium-bearing source mineral, and quartz, which is one of the most common minerals in the crust. Ar partitioning between phlogopite (a reasonable analog for biotites, though Fe–Mg content may affect partitioning [8]) and a hydrous fluid such as might characterize a wetted metamorphic pore space is in the range $K_{biot} = 10^{-4}$ to 10^{-5} [8]. Ar partitioning between quartz and biotite may be calculated by comparing Ar solubilities in the two minerals measured in the same environment (i.e. saturated within a pure Ar gas of fixed pressure). Using experimentally measured values of 1.8 ppb/bar for phlogopite [8,35] and 3.75 ppb/bar for quartz [8,36] gives a quartz/biotite partitioning of 2.1. Fig. 9 shows the TLSC of a system as a function of fluid porosity and as quartz (sink mineral) mode. As expected, for high porosities (10^{-3} or higher) the system is dominated by the fluid and

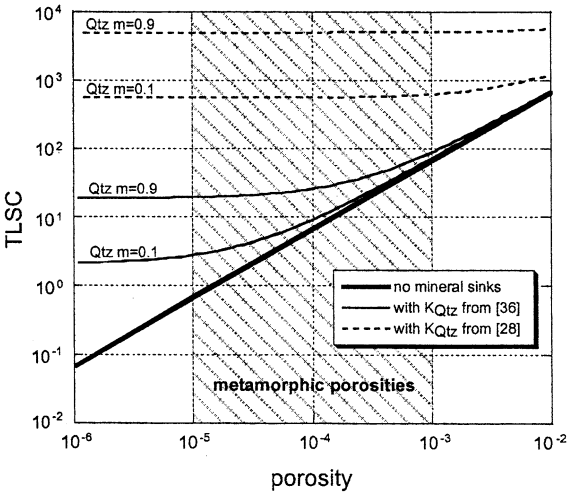

Fig. 9. Effect of porosity and quartz on TLSC. These relations are for a system with biotite source mineral mode = 0.1 and using an average K_{biot} of 5×10^{-5} derived from [8]. The heavy black line is the case for a system with only the ITM as a local sink. Light solid lines are for the addition of quartz of mode either 0.1 or 0.9 using K_{qtz} derived from [36]. Light dashed lines use K_{qtz} derived from [28]. The shaded area indicates the range of possible metamorphic porosities [24–26].

the addition of quartz has little effect on the TLSC (and thus the excess ^{40}Ar in the biotite). However, for smaller porosities (10^{-4} or lower) the system may in fact be dominated by quartz. In extreme cases, the presence of ubiquitous quartz may increase the TLSC by two or more orders of magnitude, and consequently slow the buildup of excess ^{40}Ar in system biotites by two or more orders of magnitude.

Another recent study of Ar solubility in quartz [28] suggests solubilities of ~2000 ppb/bar – more than 500 times greater than the previous measurement [36]. If the quartz/biotite partitioning of Ar is as high as suggested by considering the Watson and Cherniak [28] quartz data and the Roselieb et al. [35] phlogopite data, then quartz will dominate over both pore fluids and biotite in *any* metamorphic system where all three are present (Fig. 9). Given the significant difference in the Ar solubility for quartz from these studies – manifested in part by differences in analytical procedures (for discussion, see [28]) – it is difficult to assess the partitioning between quartz and oth-

er minerals, particularly when ratioing data which is derived from different techniques. Solubility data on biotite is equally limited and variable. An earlier study of biotite Ar solubility [37] suggested values orders of magnitude higher than the more recent value [35] (which itself is only available in an abstract), though this earlier result may reflect an artifact of air contamination [8]. Even given these uncertainties, if either the Roselieb et al. [36] or Watson and Cherniak [28] data are used, the conclusion is that quartz (or any mineral sink with similarly strong partitioning) will be a key sink for Ar in many crustal systems, with reference to biotite and other minerals with even lower solubility (e.g. K-spar [8]). It is conceivable that quartz – a common mineral in potassium-rich metapelites or metagranites frequently chosen for K/Ar geochronology – plays *the* key role in helping to prevent excess ^{40}Ar in neighboring potassium-rich minerals thus permitting successful thermochronology. Quartz poor rocks may have to rely on other sink minerals or the ITM to increase TLSC, or have very small τ_T, otherwise excess ^{40}Ar will result [6].

What other matrix minerals would be good sink candidates? Plagioclase is a ubiquitous mineral in the crust, however preliminary solubility data [8] suggest that Ar would partition weakly into plagioclase compared to biotite and most other minerals. No published partitioning data currently exist for amphibole, though given its relatively high closure temperature, it cannot constitute an effective sink for much of the lower temperature portion of the crust. Garnet, staurolite, aluminosilicates, and pyroxenes are other common crustal minerals that would be worth investigating in terms of their potential sink capacity for Ar.

Even less is known about He solubilities in the relevant phases [2]. As U–Th/He dating continues to develop, such solubility data will aid in assessing TLSC for He, and hence the extent to which excess ^{4}He is something we need to worry about.

7. Values of τ_T in natural crustal systems

τ_T may range significantly depending on L, which could be centimeters, meters or more. D^* may vary as a function of K, ϕ, and D_{ITM} as temperature, fluid chemistry, ITM interconnectivity or tortuosity change. Little is known about the actual values of D^*_{Ar} that may characterize natural systems – indeed, further measurements of this sort are a resultant suggestion stemming from this study. Recent analysis [6] of a biotite-bearing amphibolite near Simplon Pass, Switzerland, revealed $D^{Ar}_{eff} = 2.2 \pm 1.0 \times 10^{-8}$ m^2 yr^{-1} ($D^{Ar}_{eff} = D_{ITM}\phi/K_{sm}$), which, for a source mineral mode of 0.1 and density of 3 g cm^{-3}, gives $D^*_{Ar} = 7.3 \times 10^{-8}$ m^2 yr^{-1}. The extent to which this value is (or is not) representative of the average crust is unknown, but it provides a basis for discussion. τ_T, therefore, could range from 1.4×10^3 yr for $L = 1$ cm to 1.4×10^9 yr for $L = 10$ m, the latter extreme implying 700 million years worth of excess Ar buildup if steady state were ever reached. Fig. 9 shows that TLSC may range from near zero to many thousands, depending on mineralogy and fluid content. Whether or not steady-state levels of excess Ar accumulation are reached depends on TLSC (see Eq. 11), and on the amount of time the system has available to evolve before mineral closure. Typically the latter in a metamorphic environment would not be more than tens of millions of years. Thus, the maximum amount of internally derived excess Ar that may accumulate during a single metamorphic episode could be tens of millions of years' age equivalent. That amount certainly represents a significant error for many applications, particularly for younger rocks. Minerals may exhibit even greater levels of excess Ar if they have been affected additionally by inherited Ar from pre-metamorphic accumulation, or by the addition of excess Ar from external sources.

8. General applications

The physical model presented here – particularly the role of the rock system (i.e. τ_T and TLSC) – may be used to help explain or model several noble gas-related phenomena in the solid earth. Here are some examples.

- A recent study [21] showed that phlogopites

from a mantle xenolith, which had resided at temperatures hundreds of degrees above the phlogopite closure temperature, recorded an ancient Ar/Ar age far in excess of the time it was erupted and cooled through its closure temperature. This is consistent with large τ_T in the mantle environment, and/or small TLSC (i.e. little melt fraction, and/or insignificant sink minerals as suggested in [21]). In general, interpretations of xenolith noble gas data in terms of the mantle environments (i.e. τ_T and TLSC) from which they were derived [15] may be augmented by considering the model presented here.

- Systematic differences in Ar/Ar ages measured in biotites from contacting amphibolite and pelite lithologies in the Alps [6] are consistent with differing TLSC: high TLSC (and/or short τ_T) in the pelite (likely due to its quartz) vs. small TLSC in the amphibolite. Changes in amphibolite τ_T during exhumation were also linked to changing rheology and/or tectonic regime [6].
- The release and recycling of noble gases within subduction zones [14] will depend on where the radiogenic noble gases initially reside (including non-potassium (or non-U,Th minerals) for ^{40}Ar (or ^{4}He)) in subducted components and on the relevant TLSC and τ_T (i.e. distance to high transmissivity fractures or the mantle wedge).
- The model may aid the interpretation of $^{4}He/^{40}Ar$ data to constrain crustal heat or fluid flow [13], in terms of τ_T and TLSC of the systems from which the noble gases were released.

9. Conclusion: implications for geochronology

The generalized model presented here quantitatively explains the amount of internally derived excess ^{40}Ar (or ^{4}He) in a geologic system. Systems characterized by large τ_T will have a greater potential to house excess ^{40}Ar in their constituent minerals. Systems with higher TLSC will evolve more slowly towards – and perhaps never reach – their maximum steady state levels of excess ^{40}Ar. We can use these models to help predict the amount of excess ^{40}Ar in the potassium-bearing phases of interest to geochronology. That is, if we can determine τ_T and TLSC, we can predict the amount of excess ^{40}Ar. Generally, if a standard cooling age is the goal, problematic quantities of excess ^{40}Ar may be avoided by sampling from a system with short τ_T and/or high TLSC. Conversely, if we have some measure of the amount of excess ^{40}Ar (from an independent age estimate) then we can put limits on τ_T and TLSC, thereby learning more about the characteristics of that rock unit and its evolution. In this way, excess Ar can become a useful phenomenon.

Further experimental or field-based constraints on K_i and D_i for *all* common crustal minerals are particularly important. Sink mineral diffusivities are particularly apropos when interpreting noble gas contents measured today. A mineral with little or no ^{40}Ar in it today does not necessarily mean it failed to house significant ^{40}Ar deeper within the crust. Measurements of natural quartz [34,38–42], often (though not always) reveal low radiogenic ^{40}Ar content despite the likelihood discussed above that it played an important role at higher temperatures. Even small amounts of ^{40}Ar preserved in 'leaky' sink minerals like quartz could be useful in tracing the evolution of a system in terms of low-temperature τ_T, cooling rate, and in ideal situations, perhaps as a sensitive low-temperature thermochronometer.

As mentioned at the outset, the general physical model and the equations presented in this paper are directly applicable to the U–Th/He thermochronometer. The same effects of the system τ_T and TLSC, with respect to He transport and partitioning, will apply. When interpreting $^{40}Ar/^{39}Ar$ or U–Th/He thermochronologic data, the possible implications of the corresponding τ_T and TLSC for excess ^{40}Ar or ^{4}He, respectively, must be evaluated.

Acknowledgements

The author thanks Chris Ballentine, Simon Kelley and Frank Richter for thorough reviews, and Bernie Wood for editorial handling. Discussions with Simon Kelly, Terry Plank, Frank Richter, and Guido Salvucci were also helpful and appreciated. During early stages of work, E.F.B. was

supported by NSF Grant EAR-0125784 to Ken Farley and Paul Asimow of Caltech and computing facilities were provided by Paul Asimow. The bulk of this work was supported by start-up funds to E.F.B. from Boston University. *[BW]*

References

[1] I. McDougall, T.M. Harrison, Geochronology and Thermochronology by the $^{40}Ar/^{39}Ar$ Method, 2nd edn., Oxford University Press, New York, 1999, 269 pp.

[2] K.A. Farley, (U-Th)/He Dating: Techniques, calibrations, and applications. in: D. Porcelli, C.J. Ballentine, R. Weiler (Eds.), Noble Gases in Geochemistry and Cosmochemistry, Rev. Min. Geochem. 47 (2002) 819–844.

[3] E. Kirby, P.W. Reiners, M.A. Krol, K.X. Whipple, K.V. Hodges, K.A. Farley, W.Q. Tang, Z.L. Chen, Late Cenozoic evolution of the eastern margin of the Tibetan Plateau: Inferences from Ar-40/Ar-39 and (U-Th)/He thermochronology, Tectonics 21 (2002) art. 1001.

[4] M.A. House, B.P. Wernicke, K.A. Farley, Dating topographic uplift of the Sierra Nevada, California, using apatite (U-Th)/He ages, Nature 396 (1998) 66–69.

[5] M.H. Dodson, Closure temperature in cooling geochronological and petrological systems, Contrib. Mineral. Petrol. 40 (1973) 259–274.

[6] E.F. Baxter, D.J. DePaolo, P.R. Renne, Spatially correlated anomalous $^{40}Ar/^{39}Ar$ 'Age' variations about a lithologic contact near Simplon Pass, Switzerland: A mechanistic explanation for excess Ar, Geochim. Cosmochim. Acta 66 (2002) 1067–1083.

[7] S.P. Kelley, K-Ar and Ar-Ar dating. in: D. Porcelli, C.J. Ballentine, R. Weiler (Eds.), Noble Gases in Geochemistry and Cosmochemistry, Rev. Min. Geochem. 47 (2002) 785–818.

[8] S.P. Kelley, Excess argon in K-Ar and Ar-Ar geochrohnology, Chem. Geol. 188 (2002) 1–22.

[9] J.M. Eiler, L.P. Baumgartner, J.W. Valley, Intercrystalline stable isotope diffusion: a fast grain boundary model, Contrib. Mineral. Petrol. 112 (1992) 543–557.

[10] J.M. Eiler, J.W. Valley, L.P. Baumgartner, A new look at stable isotope thermometry, Geochim. Cosmochim. Acta 57 (1993) 2571–2583.

[11] G.R.T. Jenkin, G. Rogers, A.E. Fallick, C.M. Farrow, Rb-Sr closure temperatures in bi-mineralic rocks: a mode effect and test for different diffusion models, Chem. Geol. 122 (1995) 227–240.

[12] G.R.T. Jenkin, Do cooling paths derived from mica Rb-Sr data reflect true cooling paths?, Geology 25 (1997) 907–910.

[13] C.J. Ballentine, P.G. Burnard, Production, release and transport of noble gases in the continental crust. in: D. Porcelli, C.J. Ballentine, R. Weiler (Eds.), Noble Gases in Geochemistry and Cosmochemistry, Rev. Min. Geochem. 47 (2002) 481–538.

[14] D.R. Hilton, T.P. Fischer, B. Marty, Noble gases and volatile recycling at subduction zones. in: D. Porcelli, C.J. Ballentine, R. Weiler (Eds.), Noble Gases in Geochemistry and Cosmochemistry, Rev. Min. Geochem. 47 (2002) 319–370.

[15] T.J. Dunai, D. Porcelli, Storage and transport of noble gases in the subcontinental lithosphere. in: D. Porcelli, C.J. Ballentine, R. Weiler (Eds.), Noble Gases in Geochemistry and Cosmochemistry, Rev. Min. Geochem. 47 (2002) 371–409.

[16] K.A. Foland, Limited mobility of argon in a metamorphic terrain, Geochim. Cosmochim. Acta 43 (1979) 793–801.

[17] J.C. Roddick, R.A. Cliff, D.C. Rex, The evolution of excess argon in alpine biotites - a $^{40}Ar/^{39}Ar$ analysis, Earth Planet. Sci. Lett. 48 (1980) 185–208.

[18] T.M. Harrison, I. McDougall, Excess ^{40}Ar in metamorphic rocks from Broken Hill, New South Wales: Implications of $^{40}Ar/^{39}Ar$ age spectra and the thermal history of the region, Earth Planet. Sci. Lett. 55 (1981) 123–149.

[19] R.J. Cumbest, E.L. Johnson, T.C. Onstott, Argon composition of metamorphic fluids: Implications for $^{40}Ar/^{39}Ar$ geochronology, Geol. Soc. Am. Bull. 106 (1994) 942–951.

[20] S. Scaillet, Excess ^{40}Ar transport scale and mechanism in high-pressure phengites: a case study from an eclogitized metabasite of the Dora-Maira nappe, western Alps, Geochim. Cosmichim. Acta 60 (1996) 1075–1090.

[21] S.P. Kelley, J.-A. Wartho, Rapid kimberlite ascent and the significance of Ar-Ar ages in xenolith phlogopites, Science 289 (2000) 609–611.

[22] E.F. Baxter, D.J. DePaolo, Field measurement of bulk metamorphic reaction rates I: Theory and technique, Am. J. Sci. 302 (2002) 442–464.

[23] J. Selverstone, G. Morteani, J.M. Staude, Fluid channeling during ductile shearing: transformation of granodiorite into aluminous schist in the Tauern Window, Eastern Alps, J. Met. Geol. 9 (1991) 419–431.

[24] G.M. Dipple, J.M. Ferry, Metasomatism and fluid flow in ductile fault zones, Contrib. Mineral. Petrol. 112 (1992) 149–164.

[25] J.J. Ague, Mass transfer during Barrovian metamorphism of pelites, south-central Connecticut, II: Channelized fluid flow and the growth of staurolite and kyanite, Am. J. Sci. 294 (1994) 1061–1134.

[26] M. Grove, T.M. Harrison, $^{40}Ar^*$ diffusion in Fe-rich phlogopite, Am. Mineral. 81 (1996) 940–951.

[27] T.M. Harrison, Diffusion of ^{40}Ar in hornblende, Contrib. Mineral. Petrol. 78 (1981) 324–331.

[28] E.B. Watson, D.L. Cherniak, Lattice diffusion of Ar in quartz, with constraints on Ar solubility and evidence of nanpores, Geochim. Cosmocim. Acta 67 (2003) 2043–2062.

[29] D.J. DePaolo, S.R. Getty, Models of isotope exchange in reactive fluid-rock systems: Implications for geochronology in metamorphic systems, Geochim. Cosmochim. Acta 60 (1996) 3933–3947.

[30] J. Crank, The Mathematics of Diffusion, Clarendon Press, Oxford, 1975, 414 pp.
[31] J.V. Walther, B.J. Wood mineral fluid reaction rates. in: J.V. Walther, B.J. Wood (Eds.), Fluid-Rock Interactions During Metamorphism, Springer, New York, 1986, pp. 194–212.
[32] R.B. Hanson, Hydrodynamics of regional metamorphism due to continental collision, Econ. Geol. 92 (1997) 880–891.
[33] T. Hiraga, O. Nishikawa, T. Nagase, M. Akizuki, Morphology of intergranular pores and wetting angles in pelitic schists studied by transmission electron microscopy, Contrib. Mineral. Petrol. 141 (2001) 613–622.
[34] S. Sherlock, S.P. Kelley, Excess argon evolution in HP-LT rocks: a UVLAMP study of phengite and K-free minerals, NW Turkey, Chem. Geol. 182 (2002) 619–636.
[35] K. Roselieb, J.-A. Wartho, H. Buttner, A. Jambon, S.P. Kelley, Solubility and diffusivity of noble gases in synthetic phlogopite: a UV LAMP investigation, Terra Abstr. 4 (1999) 368.
[36] K. Roselieb, P. Blanc, H. Buttner, A. Jambon, W. Rammensee, M. Rosenhauer, D. Vielzeuf, H. Walter, Experimental study of argon sorption in quartz: Evidence for argon incompatibility, Geochim. Cosmochim. Acta 61 (1997) 533–542.
[37] T.C. Onstott, D. Phillips, Pringle-Goodell, Laser microprobe measurement of chlorine and argon zonation in biotite, Chem. Geol. 90 (1991) 145–168.
[38] N.O. Arnaud, S.P. Kelley, Evidence for excess argon during high pressure metamorphism in the Dora Maira Massif (western Alps, Italy) using ultra-violet later ablation microprobe ^{40}Ar-^{39}Ar technique, Contrib. Mineral. Petrol. 121 (1995) 1–11.
[39] S.M. Reddy, S.P. Kelley, L. Magennis, A microstructural and argon laserprobe study of shear zone development at the western margin of the Nanga Parbat-Haramosh Massif, western Himalaya, Contrib. Mineral. Petrol. 128 (1997) 16–29.
[40] J.F. Evernden, Early developments (1952–1965) in K-Ar geochronology at Berkeley, Geol. Soc. Am. Cordill. Sect. Abstr. Prog. 31 (1999) A-53.
[41] H. Qiu, 40Ar-39Ar dating of the quartz samples from two mineral deposits in western Yunnan (SW China) by crushing in vacuum, Chem. Geol. 127 (1999) 211–222.
[42] D. Vance, M. Ayres, S.P. Kelley, N. Harris, The thermal response of a metamorphic belt to extension: constraints from laser Ar data on metamorphic micas, Earth Planet. Sci. Lett. 162 (1998) 153–164.